Behavior Problems After Early Life Stress: Contributions of the Hippocampus and Amygdala

Supplemental Information

Sample Characteristics

Children in the early neglect group were adopted from Romania (n = 16), Russia (n = 10), China (n = 6), and Bulgaria (n = 2). Parents for two children did not report a country of origin for their adopted child.

Poverty was classified using the Hollingshead Inventory, which codes parental education and occupation on a seven-point scale ranging from 1 (higher executives, major professionals; professional degree) to 7 (unskilled employees; less than seven years of school). Child poverty was defined as a score of 50 or less on the Hollingshead Inventory.

Pubertal Examination Procedures

Experienced pediatric nurse practitioners conducted physical examinations for research purposes (S1). The clinical examination for girls assessed breast development with brief palpation and visual examination of pubic hair. An orchidometer was used to measure testicular size in boys (S2), along with visual inspection of pubic hair. Interobserver reliability between the nurse practitioners (n = 10) was good, $\kappa = 0.88$. Puberty was rated ranging from 1 (no development) to 5 (adult development) (S3, S4).

Fetal Alcohol Screen

All children were screened for fetal alcohol exposure due to the heightened risk in the children exposed to early neglect. Digital pictures of all participants were analyzed using Fetal

Alcohol Syndrome Facial Photographic Analysis Software (S5). This system assesses (a) distance between the endocanthion and exocanthion landmarks, (b) philtrum smoothness, and (c) upper lip thinness. This screening tool has demonstrated very high sensitivity and specificity for prenatal alcohol exposure (S6). A medical geneticist who specializes in fetal alcohol syndrome also reviewed facial photographs of all participants. No children from any group had signs of fetal alcohol exposure or fetal alcohol syndrome.

Magnetic Resonance Imaging Methods

All MRI images were acquired on 3-Tesla GE SIGNA (General Electric Medical Systems, Waukesha, Wisconsin) with a quadrature head coil. A three-dimensional, inversion recovery pulse sequence was used to generate T1-weighted images with the following parameters: TR/TE = 21/8 ms, flip angle = 308, 240 mm field of view, 256-192 in-plane acquisition matrix (interpolated on the scanner to 256-256), and 128 axial slices (1.2 mm thick) covering the whole cerebrum. Following acquisition, images were bias corrected to smooth field inhomogeneities, underwent skull and vessel correction, were contrast-adjusted, and were reoriented to the pathological plane.

Amygdala Region of Interest Drawing

Volume of interest (VOI) drawing of the amygdala was based on the criteria detailed in Nacewicz and colleagues (S7). Tracing started in the most superior plane in which gray matter was present lateral to the optic tract, posteromedial to the anterior commissure, and anteromedial to the optic radiations. Working inferiorly, a tangent to the anteromedial extent of the optic tract defined the posterolateral border. Initial separation of the medial amygdala from the

hippocampus was by linear extension of the posterior amygdala–cerebrospinal fluid border, but more precise separation was reserved for coronal sections. An arc extending anteriorly and medially from the temporal lobe white matter and following its curvature formed the anterolateral border. More inferiorly, the anterolateral border was approximated, but exclusion of other mesial temporal structures was achieved in the coronal view. Superiorly, the anterior border extended as far as the middle cerebral artery. More inferiorly, the medial and anterior amygdala was separated from the entorhinal cortex.

Regions were then refined through plane-by-plane comparison with ex-vivo atlas sections. Tracing at the most posterior coronal section in which gray matter was present as the lateral roof of the inferior horn. While white matter formed the superolateral border, a tangent to the optic tract defined the superomedial extent. Moving anteriorly, the close approximation of the anterior commissure to the amygdala was exploited to exclude the caudate: regions of interest never extended between the superomedial extent of the temporal lobe white matter and the more lateral of the medial edge of the anterior commissure or the lateral extent of the collateral sulcus. Working medially, separation from the hippocampus, optic radiations, caudate/putamen, and entorhinal cortex was confirmed in the sagittal view. Regions were refined until surfaces were smooth to ensure agreement in all planes. Example axial and coronal MRI slices with tracing overlays are shown in Figures S1-S2.

Hippocampal Region of Interest Drawing

Hippocampal VOIs were traced based on the criteria detailed in Ref. S8. Tracing began in the sagittal plane where the gray matter of the entire hippocampus was easily identified running inferiorly to the temporal horn of the lateral ventricle, and otherwise surrounded by white matter.

Axial and coronal views were used to refine the initial VOI, though final corrections were done in the coronal plane. Starting in the sagittal view, the anterior hippocampus was differentiated from the amygdala by the white matter of the alveus. The superior border was defined by the temporal horn of the lateral ventricle and white matter superior to temporal cortex provided an inferior border. The posterior border was defined by the trigone of the lateral ventricle and white matter immediately inferior to the ventricle. Further refinement continued in all three views, with the coronal view providing the most informative comparison with the atlases. Coronally, the anterior hippocampus was drawn either inferior to or adjacent to the anterior portion of the temporal horn of the lateral ventricle, which also provided the lateral border. The medial border was identified by the shape of the white matter of the parahippocampal gyrus, forming a "V" inferior to the hippocampus. The uncus was included in the hippocampal VOI when the uncul sulcus began to extend medially into the ambient cistern. The superior border of the hippocampus was differentiated from the amygdala by following, medially, the arch of lateral ventricle. The superior border was also informed by either following (and including) the white matter of the alveus or using an approximated horizontal line starting at the superior edge of the temporal horn of the lateral ventricle, extending medially through to the ambient cistern. The inferior border was identified by white matter differentiating hippocampus from the parahippocampal gyrus. When identifying the most posterior aspect of the hippocampus, the crus of the fornix, fasciolar gyrus, Andreas Retzius gyrus, fasciola cinerea, and gyrus fasciolaris were included. These structures were differentiated from the pulvinar complex of the thalamus by the difference in gray scale, as the thalamus is a paler shade of gray. Example axial and coronal MRI slices with tracing overlays are shown in Figures S1-S2.

Information about Cumulative Life Stress Scores

To detail specific examples from our study, a score of a 1 was given to a child whose pet was hit by a car, but was not seriously injured. A score of a 5 was given to a child who was in foster care early in life, had multiple moves, and also had one of their parents die early in life. A score of a 10 was given to a child who was homeless, had several close family members die unexpectedly, and whose parents had a highly conflictual relationship that resulted in separation.

Descriptive Statistics on Early Life Stress (ELS) and Behavioral Dysregulation

Similar to previous reports, all forms of ELS were each associated with behavioral dysregulation. Specifically, children exposed to early neglect (t = 3.429, p < .001), extreme poverty (t = 2.661, p = .01), or physical abuse (t = 5.24, p < .001) had significantly greater behavioral problems than comparison children without a history of adversity. Comparable patterns also were found when looking at cumulative levels of stress exposure, with greater levels of stress associated with more behavioral dysregulation (r = .382, p < .001).

Group Differences When Controlling For Age

To probe group differences in medial temporal lobe, right and left volumes for each structure were entered separately into linear regressions as dependent variables. Total gray matter, sex (as a dummy coded variable), puberty, and group (as a dummy coded variable) were entered as independent variables. Regression analyses indicated that children who suffered early neglect had smaller left amygdala volumes relative to comparison children (β = -.239, t = -2.031, p = .046). Children from low socioeconomic status (SES) households had smaller left amygdala volumes (β = -.395, t = -3.137, p = .003) relative to comparison children. Smaller left

(β = -.294, t = -2.348, p =.027) and right (β = -.289, t = -2.274, p = .027) hippocampal volumes also were found for children from low SES households relative to comparison children. Children who suffered physical abuse had smaller left amygdala volumes (β = -.350, t = -3.059, p = .003) relative to comparison children. Children who suffered physical abuse also showed smaller right hippocampal volumes (β = -.248, t = -2.172, p = .033), and a trend for smaller left hippocampal volumes (β = -.219, t = -1.873, p = .065).

Correlations Between Volumetric Differences and Child Behavioral Reports

Here we performed a sensitivity check, recomputing correlations between volumetric differences and child reports of behavior problems. Similar to the results using a consensual rating, greater behavior problems such as disobeying rules were associated with smaller left amygdala volumes (r = -.213, p = .018) and smaller hippocampal volumes (Left r = -.235, p = .008; Right r = -.254, p = .004) across the full sample.

Automated Quantification of the Amygdala

For comparison purposes, segmentation of the amygdala was also performed for all subjects in the Freesurfer image analysis suite, which is documented and freely available for download online (http://surfer.nmr.mgh.harvard.edu/). Briefly, this processing includes motion correction, removal of non-brain tissue using a hybrid water- shed/surface deformation procedure, automated Talairach transformation, segmentation of the subcortical white matter, and subcortical volumetric structures (including the amygdala; S9, S10).

Statistical Analyses using Automatically Derived Amygdala Segments

Employing similar regression models to the ones described previously, we examined group differences and behavioral correlations with automatically segmented amygdala volumes (in place of hand-traced values). In contrast to statistical estimates derived from hand-quantification, no differences were found when investigating specific types of early adversity. Freesurfer derived left amygdala volumes for children who suffered early neglect (t = -1.143, p = .257), who suffered physical abuse (t = -1.493, p = .14), or living in extreme poverty (t = -1.346, p = .184) were not significantly different than comparison children. Correlations between behavioral dysregulation and automatically-segmented left amygdala volumes were also not significant (r = -.072, p = .508).

Table S1. Sample Demographic Information.

	Group			
	Comparison (without ELS)	**Early Neglect**	**Low SES**	**Physically Abused**
Sex	15 females, 26 males	21 females; 15 males	14 females; 6 males	11 females; 20 males
Age (Months)	140.46 ± 21.57 months	139.34 ± 20.2 months	146.24 ± 20.15 months	143.13 ± 20.0 months
Puberty[1]	1.37 ± 1.14	1.41 ± 1.12	2.51 ± 1.24	1.75 ± 1.09
SES[2]	56.04 ± 5.86	53.42 ± 8.64	31.89 ± 10.10	30.19 ± 9.68
Behavior Problems[3]	1.56 ± 0.68	2.29 ± 1.15	2.29 ± 1.11	2.63 ± 1.04
Cumulative Stress Exposure[4]	2.56 ± 1.34	5.13 ± 2.19	5.05 ± 2.37	6.86 ± 2.09

ELS, early life stress; socioeconomic status; YLSI, Youth Life Stress Interview.

[1] As measured by Tanner Staging, ranging from 1 (no development) to 5 (adult development).

[2] Using the Hollingshead Inventory where 20=Parents are unskilled laborers such as custodial staff and have less than a high school education, 30=Parents have sales positions and have a high school education (or have completed some college), and 40=Both parents have high skilled jobs such as managers and have completed college (or additional professional schooling).

[3] Using the YLSI, score range 1-5.

[4] Also using the YLSI, score range 1-10.

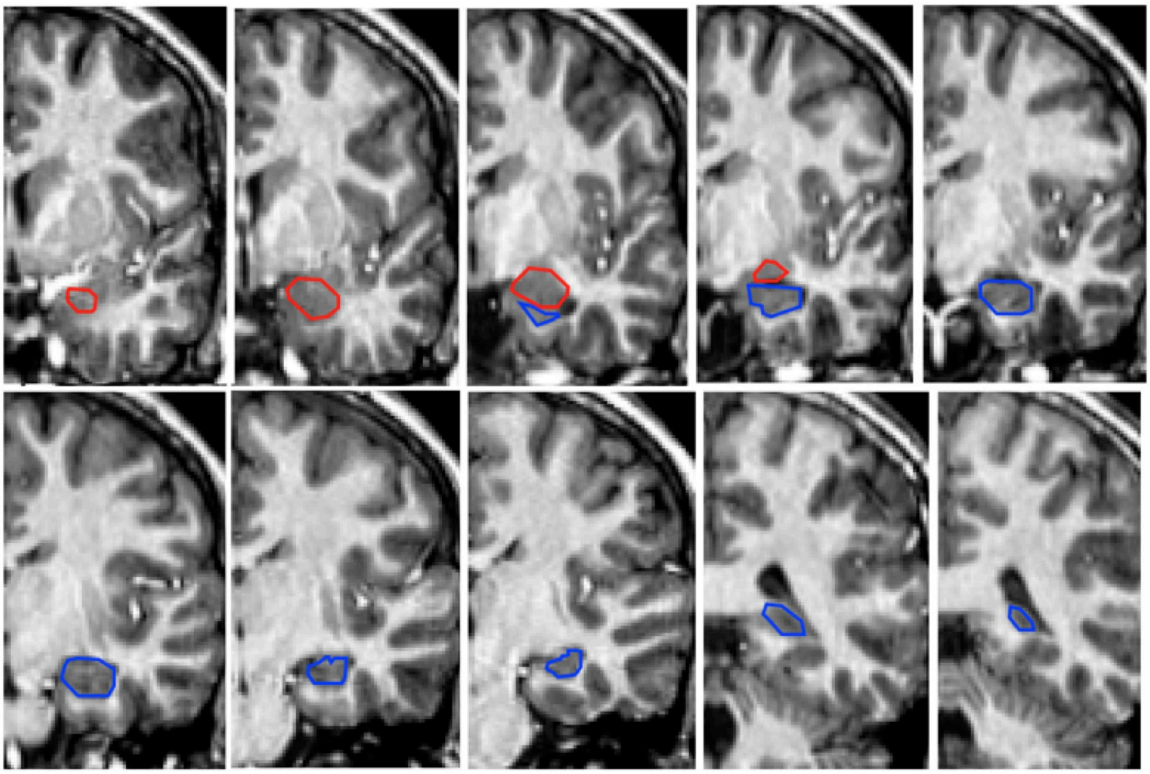

Figure S1. Figure S1 shows coronal slices of amygdala and hippocampal region of interest drawing. The amygdala is shown in red, while the hippocampus is shown in blue. The top left corner shows more anterior regions of the brain, with the neighboring sections showing more posterior slices. The most posterior slice is shown in the bottom right corner.

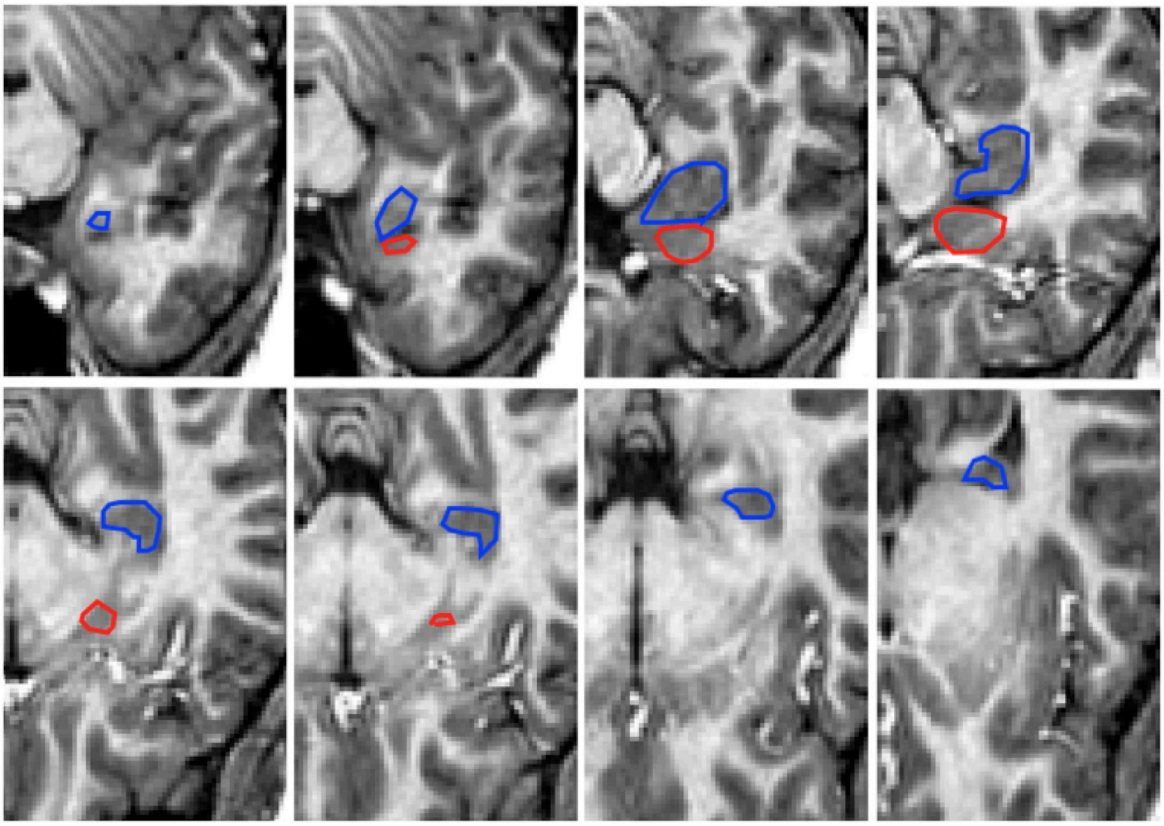

Figure S2. Figure S2 shows axial slices of amygdala and hippocampal region of interest drawing. The amygdala is shown in red, while the hippocampus is shown in blue. The top left corner shows more inferior regions of the brain, with the neighboring sections showing more superior slices. The most superior slice is shown in the bottom right corner.

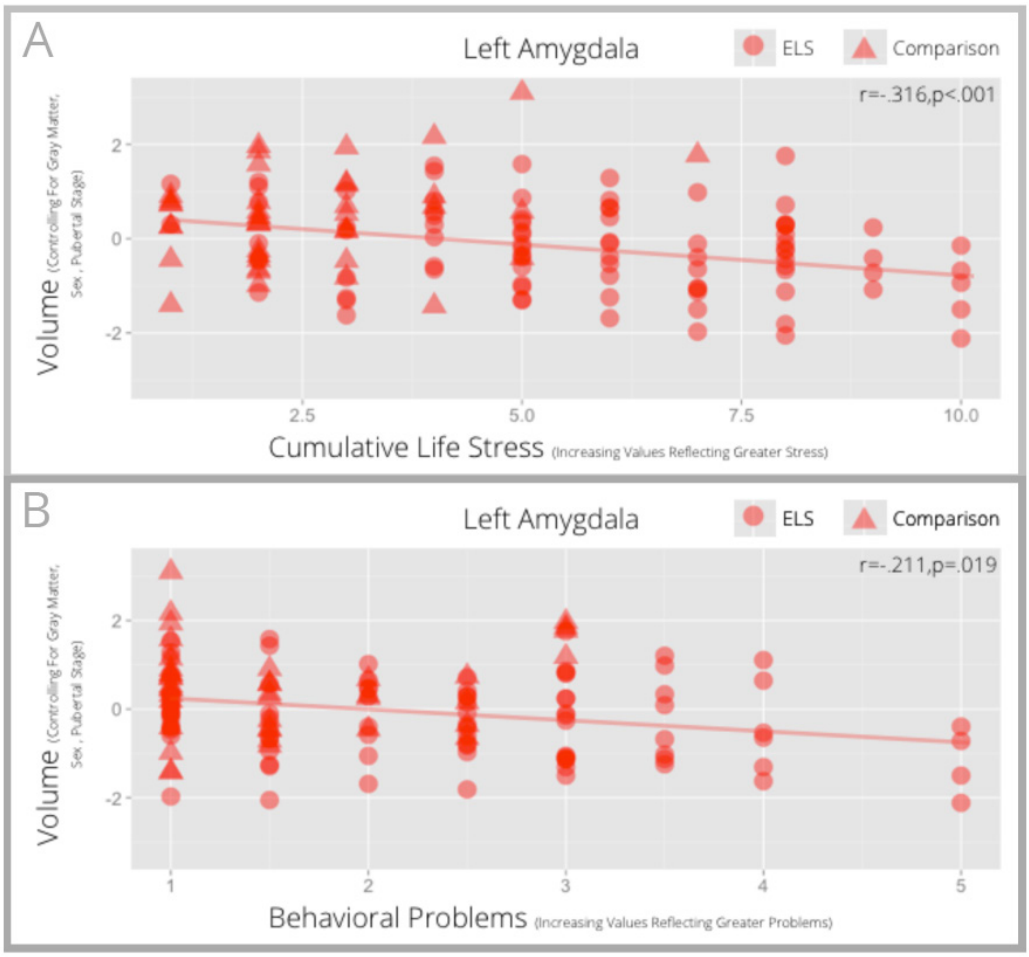

Figure S3. Scatterplots between left amygdala volume and cumulative stress exposure (**A**) and behavioral problems (**B**) for all participants are shown in this figure. Participants who had experienced early life stress (ELS) are depicted as circles, while participants without a history of ELS are depicted as triangles. Standardized residuals of amygdala volume controlling for total gray matter, pubertal stage, and gender (dummy coded) are shown on the vertical axis while cumulative stress exposure (**A**) or behavioral problems (**B**) is shown on the horizontal axis.

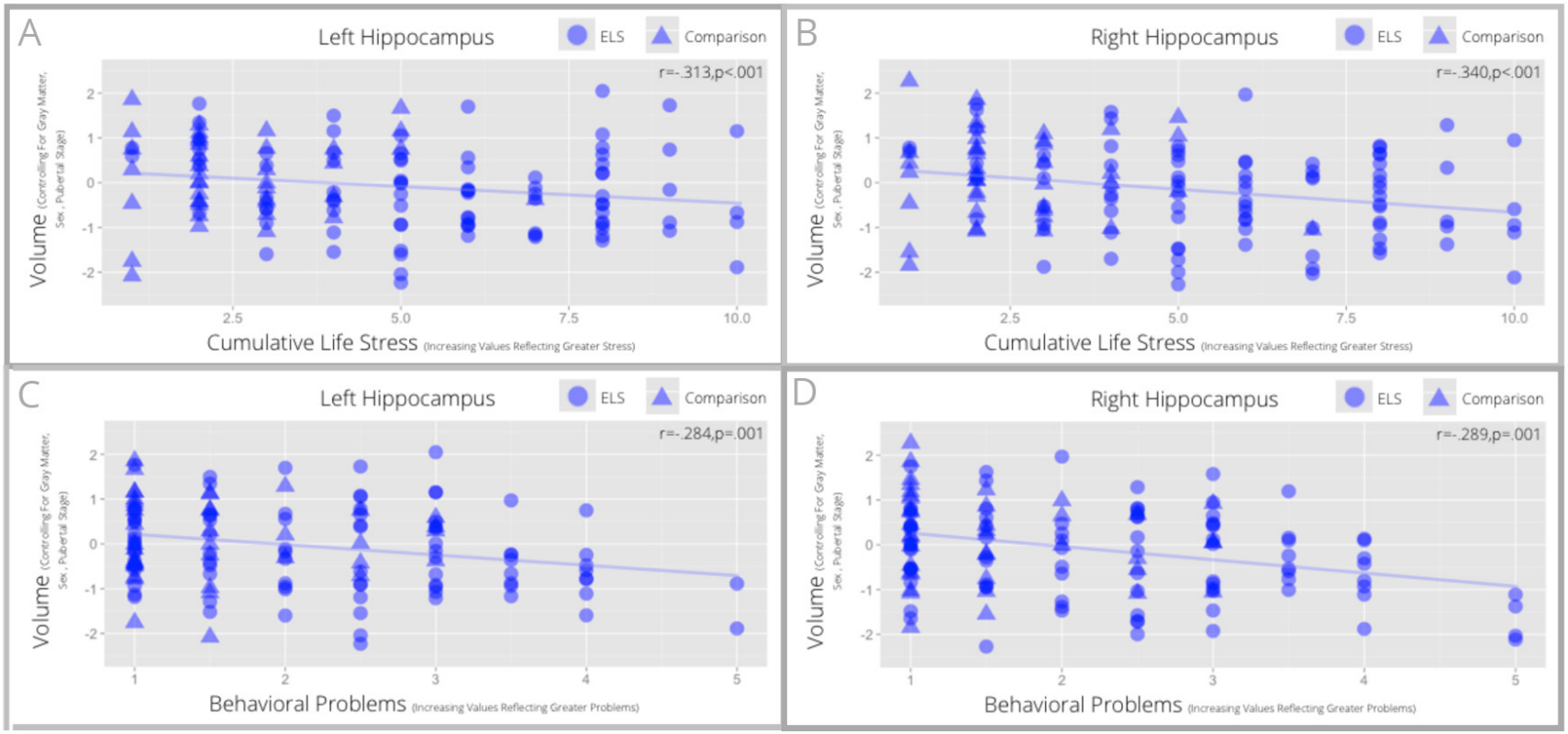

Figure S4. Scatterplots between hippocampal volume and cumulative stress exposure (Left Hippocampus Panel **A**; Right Hippocampus Panel **B**) and behavioral problems (Left Hippocampus Panel **C**; Right Hippocampus Panel **D**) for all participants are shown in this figure. Participants who had experienced early life stress (ELS) are depicted as circles, while participants without a history of ELS are depicted as triangles. Standardized residuals of hippocampal volume controlling for total gray matter, pubertal stage, and gender (dummy coded) are shown on the vertical axis while cumulative stress exposure (**A** and **B**) or behavioral problems (**C** and **D**) is shown on the horizontal axis.

Supplemental References

S1. Shirtcliff EA, Dahl RE, Pollak SD (2009): Pubertal development: correspondence between hormonal and physical development. *Child Dev.* 80:327-337.

S2. Genentech (1997): *Assessment of pubertal stages,* G70577-R1#LF0050. San Francisco: Genentech.

S3. Marshall WA, Tanner JM (1969): Variations in pattern of pubertal changes in girls. *Arch Dis Child.* 44:291-303.

S4. Marshall WA, Tanner JM (1970). Variations in the pattern of pubertal changes in boys. *Arch Dis Child.* 45:13-23.

S5. Astley SJ (2003): *FAS facial photographic analysis soft-ware.* Version 1.0.0. [Computer software] Seattle: FAS Diagnostic & Prevention Network, University of Washington.

S6. Astley SJ, Stachowiak J, Clarren SK, Clausen C (2002): Application of the fetal alcohol syndrome facial photographic screening tool in a foster care population. *J Pediatr.* 141:712–717.

S7. Nacewicz BM, Dalton KM, Johnstone T, Long MT, McAuliff EM, Oakes TR, *et al.* (2006): Amygdala volume and nonverbal social impairment in adolescent and adult males with autism. *Arch Gen Psychiatry.* 63:1417–1428.

S8. Rusch BD, Abercrombie HC, Oakes TR, Schaefer SM, Davidson RJ (2001): Hippocampal morphometry in depressed patients and control subjects: relations to anxiety symptoms. *Biol Psychiatry.* 50:960–964.

S9. Fischl B, van der Kouwe A, Destrieux C, Halgren E, Ségonne F, Salat DH, *et al.* (2004): Automatically parcellating the human cerebral cortex. *Cereb Cortex.* 14:11–22.

S10. Fischl B, Salat DH, Busa E, Albert M, Dieterich M, Haselgrove C, *et al.* (2002): Whole brain segmentation: automated labeling of neuroanatomical structures in the human brain. *Neuron*. 33:341–355.